

MARTIN MARIETTA ENERGY SYSTEMS LIBRARIES



3 4456 0376522 7

**ornl**

ORNL/TM-12300

**OAK RIDGE  
NATIONAL  
LABORATORY**

**MARTIN MARIETTA**

**Design of an Advanced TLD-Based  
Fixed Nuclear Accident Dosimeter**

W. H. Casson, Sr.  
G. T. Mei

OAK RIDGE NATIONAL LABORATORY

CENTRAL RESEARCH LIBRARY

CIRCULATION SECTION

4500N ROOM 173

**LIBRARY LOAN COPY**

DO NOT TRANSFER TO ANOTHER PERSON

If you wish someone else to see this report, send in name with report and the library will arrange a loan.

9C929835 672

MANAGED BY  
MARTIN MARIETTA ENERGY SYSTEMS, INC.  
FOR THE UNITED STATES  
DEPARTMENT OF ENERGY

This report has been reproduced directly from the best available copy.

Available to DOE and DOE contractors from the Office of Scientific and Technical Information, P.O. Box 62, Oak Ridge, TN 37831; prices available from (615) 576-8401, FTS 626-8401.

Available to the public from the National Technical Information Service, U.S. Department of Commerce, 5285 Port Royal Rd., Springfield, VA 22161.

This report was prepared as an account of work sponsored by an agency of the United States Government. Neither the United States Government nor any agency thereof, nor any of their employees, makes any warranty, express or implied, or assumes any legal liability or responsibility for the accuracy, completeness, or usefulness of any information, apparatus, product, or process disclosed, or represents that its use would not infringe privately owned rights. Reference herein to any specific commercial product, process, or service by trade name, trademark, manufacturer, or otherwise, does not necessarily constitute or imply its endorsement, recommendation, or favoring by the United States Government or any agency thereof. The views and opinions of authors expressed herein do not necessarily state or reflect those of the United States Government or any agency thereof.

ORNL/TM-12300

407  
91

Office of Radiation Protection

**DESIGN OF AN ADVANCED TLD-BASED FIXED NUCLEAR  
ACCIDENT DOSIMETER**

**W. H. Casson, Sr.  
G. T. Mei**

**Date Completed—March 1993  
Date Published—August 1993**

**NOTICE:** This document contains information of a preliminary nature. It is subject to revision or correction and therefore does not represent a final report.

**OAK RIDGE NATIONAL LABORATORY  
Oak Ridge, Tennessee 37831-6285  
managed by  
MARTIN MARIETTA ENERGY SYSTEMS, INC.  
for the  
U.S. DEPARTMENT OF ENERGY  
under contract DE-AC05-84OR21400**



3 4456 0376522 7



# CONTENTS

	<u>Page</u>
FIGURES .....	v
TABLES .....	vii
ABSTRACT .....	1
1. INTRODUCTION .....	1
2. INSTRUMENT DESCRIPTION .....	5
3. DOSIMETER RESPONSE .....	9
4. CALCULATED RESULTS .....	13
5. EXPERIMENTAL RESULTS .....	21
6. CONCLUSIONS .....	25
REFERENCES .....	27
APPENDIX A .....	29



## FIGURES

<u>Figure</u>		<u>Page</u>
1	Configuration of the Energy Systems beta/gamma TLD dosimeter . . . . .	5
2	Configuration of the Energy Systems neutron TLD albedo dosimeter . . .	6
3	Design of fixed nuclear accident dosimeter with advanced phantom design . . . . .	7
4	Response of neutron dosimeter TLDs to monoenergetic neutrons when mounted on front of accident dosimeter as calculated by Monte Carlo code . . . . .	13
5	Response of neutron dosimeter TLD elements in center of phantom to neutrons as calculated by Monte Carlo code . . . . .	14
6	Response of neutron dosimeter TLD elements on back of phantom to neutrons as calculated by Monte Carlo code . . . . .	15
7	Total response of complex phantom design with and without additional dosimeter on back surface . . . . .	16
8	Uncollided fission spectrum (solid) with four-element response (dotted) and six-element response (dashed) . . . . .	17
9	Response of complex phantom design when combined with sulfur pellet response . . . . .	18
10	Response of TLDs at front and back positions as a function of angle . .	23
11	Response of TLDs at center position as a function of angle . . . . .	24



## TABLES

<u>Table</u>		<u>Page</u>
1	Calculational results of the six-element-plus-sulfur fixed accident dosimeter response to neutron fluence from various sources . . . . .	19
2	Calculational results of the fixed accident dosimeter response to neutron absorbed dose from various sources . . . . .	20



## ABSTRACT

A new system has been designed for use as a fixed nuclear accident dosimeter based upon the thermoluminescent dosimeter (TLD) system used for personnel dosimetry at U.S. Department of Energy facilities managed by Martin Marietta Energy Systems, Inc. The system is made up of a small phantom consisting of two main parts measuring  $20 \times 20 \times 5$  cm and made from polymethylmethacrylate. A neutron-sensitive TLD card is placed in the center between the two pieces. Also, TLD cards in standard holders are mounted on the front and back of the phantom. A derivation is made of a linear combination of the responses from the TLD elements which results in calculation of the neutron fluence, absorbed dose, and dose equivalent. By using the right linear combinations, a crude spectrum can be estimated, which allows further calculation of the average fluence-to-dose-equivalent conversion factor.

The response of the system was tested and found to be applicable for the evaluation of typical nuclear accident spectra, although considerable improvement can be made by the addition of a sulfur pellet. The system was also tested for angular dependence. In order to move the development of this system from the proof-of-principle to full application, the calculation of the TLD response curves must be improved, additional measurements must be made, and the system must be tested in a simulated accident neutron field.

The advantages of the new fixed dosimeter system are its simplicity, easy maintenance, and lower operational cost. The system uses standard TLD cards that are already in place throughout Energy Systems facilities. The TLD process personnel are familiar with evaluating doses from TLDs and can provide information necessary to ensure timely and accurate assessment of exposures that may result from criticality accidents. Most of the quality control requirements are part of the existing personnel dosimetry system. Overall, the simplification of providing a TLD-based fixed nuclear accident dosimeter unit using existing facilities minimizes resource requirements without compromising functionality or capability.



# DESIGN OF AN ADVANCED TLD-BASED FIXED NUCLEAR ACCIDENT DOSIMETER

W. H. Casson, Sr.\*  
G. T. Mei

## 1. INTRODUCTION

In the past, Fixed Nuclear Accident Dosimeters (FNADs) relied upon activation foils and threshold detector units (TDUs).<sup>1</sup> Additional detectors, such as radiophotoluminescent (RPL) glass and track-etch detectors, were used to provide supplementary information. Each component of the dosimeter often required a different analysis system, system calibration, or system setup. Some techniques were very difficult to master and required a well-trained operator to obtain reliable results. In the end, the complete analysis of an accident dose required a large investment in equipment and equipment maintenance. In the past, this was not difficult since the equipment could be used for research or left in standby until needed. In today's work environment, the equipment must be well maintained and, if part of a critical system is used as an accident dosimeter system, it should not be used for experimental applications. Also, since the amount of research being conducted with large dose irradiations is in sharp decline, the expertise available to analyze such data and to properly oversee system operation is rapidly disappearing. There is a need for an accident dosimetry system which is simple to operate and analyze, easy to maintain, and can meet all regulatory requirements.

The Personnel Nuclear Accident Dosimeter (PNAD) System implemented at Martin Marietta Energy Systems, Inc., facilities has accomplished this goal for personnel monitoring using thermoluminescent dosimeters (TLDs), assigned routinely to each employee, without modification.<sup>2</sup> Standard procedures for retrieving and processing PNADs are fully implemented. The savings to the Laboratory in equipment cost and personnel time have

---

\*Health and Safety Research Division, Oak Ridge National Laboratory, Oak Ridge, Tennessee.

been substantial. Tests conducted at the Aberdeen Proving Grounds demonstrated the ability of the PNAD to meet the requirements of DOE Order 5480.11. The analysis system is based on published neutron spectra expected during a nuclear accident. A foreknowledge of the exposure conditions will allow an estimate of the neutron spectrum and, therefore, allow analysis of the TLD data without further complex algorithms. In principle, an FNAD or neutron area monitor can function in the same manner. The FNAD, however, is also required to provide a rough neutron spectrum.<sup>3</sup>

Perhaps the most standard technique of measuring a neutron spectrum is by use of Bonner spheres.<sup>4</sup> With this technique, a neutron detector is placed within a series of polyethylene spheres of different diameters. Appropriate response curves combined with the data can be used to unfold the neutron spectrum into a large number of energy groups. With this spectral information and a knowledge of the neutron fluence, the various radiation dose quantities can be calculated. The use of TLDs inside a Bonner sphere set is one possibility for an FNAD system meeting performance requirements of the DOE Order, although the spheres (usually six to eight in number) are not practical for use in this type of application because of their physical size and cost. A single sphere, however, can provide the desired results and has been applied to neutron area monitoring applications in several European nuclear facilities.<sup>5</sup>

For detection of neutrons by direct interaction, the angle of incidence can be very important. On the other hand, if the detector is of the albedo type, or placed within a moderator, detecting primarily the scattered neutrons tends to flatten the angular response. A spherical moderator with a TLD at the center would be almost flat in angular response. Although a spherical design would be the most efficient, the outside shape of a near-spherical moderator would, at most, have only a secondary effect on TLD response. The standard (square) phantom design can be considered for use if the detector is mounted at the center of the moderator.

To determine the optimum phantom size, a series of measurements and calculations were made and compared. By taking the mass of a small volume element and dividing by the square of the distance from the element center to the detector, the relative contribution of the scattering from that element could be approximated. Summing these relative contributions over the moderator volume gave a numerical result which could be used to

estimate the contribution of moderated neutrons to the detector signal. Agreement with experimental measurements was very good. The effect of the phantom size was found not to significantly affect the results of a TLD albedo dosimeter mounted at the center of the front face until the phantom dimensions were less than  $20 \times 20 \times 10$  cm. Based on those results, phantoms of that size were used for FNADs throughout Energy Systems facilities with TLD albedo units mounted on the front face, while development work was being carried out on a modification of the phantom design to allow moderated measurements to be made. Use of the  $20 \times 20 \times 10$  cm phantom allowed convenient mounting and reduced the cost when compared to a full-size  $40 \times 40 \times 15$  cm phantom.

The system was optimized for neutron spectra from both uncollided and moderated fission neutrons which could result from an accidental nuclear excursion. Further advantage was gained by mounting a dosimeter on the back of the phantom. The basis for these investigations was experimental data gathered with several neutron source configurations at the Radiation Calibration Laboratory (RADCAL) [a radiation calibration facility at Oak Ridge National Laboratory (ORNL)]. The work was further supplemented by Monte Carlo calculations of the response functions of the dosimeters mounted at different locations with respect to the moderator. These response functions were used to develop algorithms for evaluating the results from the calibrated exposures.

The results of the calculations, tests, and algorithm development are presented here along with recommendations for implementation of a fixed accident dosimeter system based upon these data.



## 2. INSTRUMENT DESCRIPTION

The core of the FNAD system is the TLD unit used in routine personnel monitoring by the Energy Systems Centralized External Dosimetry System (CEDS) at DOE facilities in Oak Ridge. The CEDS dosimetry system consists of a beta/gamma dosimeter and a separate neutron dosimeter. The beta/gamma dosimeter (shown in Fig. 1) has three TLD-700 elements (sensitive only to beta/gamma radiation) and one TLD-600 element (sensitive both to beta/gamma radiation and to neutrons). By mounting the beta/gamma unit off-center on the front face of the phantom, the gamma component of an accident dose can be easily evaluated. The required algorithms are the same as those used for routine dosimeter evaluation.

The neutron dosimeter consists of two TLD-600/TLD-700 element pairs. One pair is mounted under 300 mg/cm<sup>2</sup> of ABS plastic and is very sensitive to thermal and low-energy neutrons (Fig. 2). The second pair is mounted under a cadmium filter which blocks most of

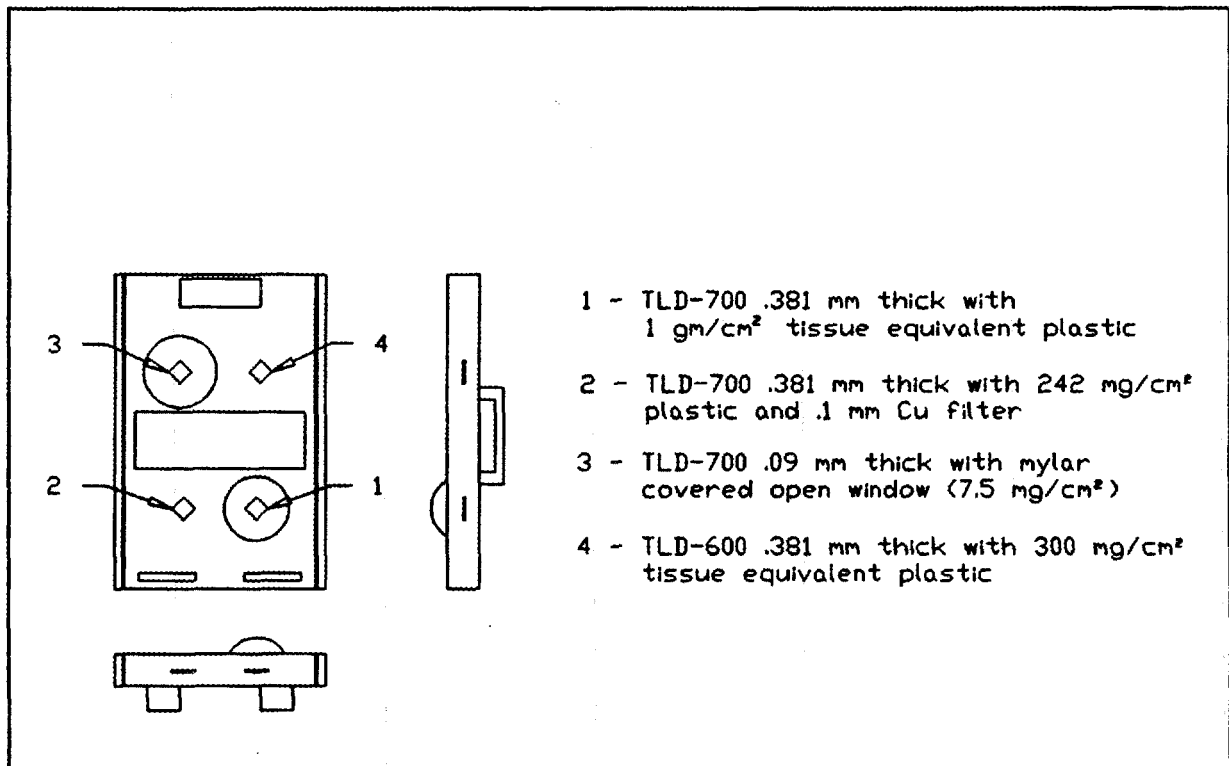
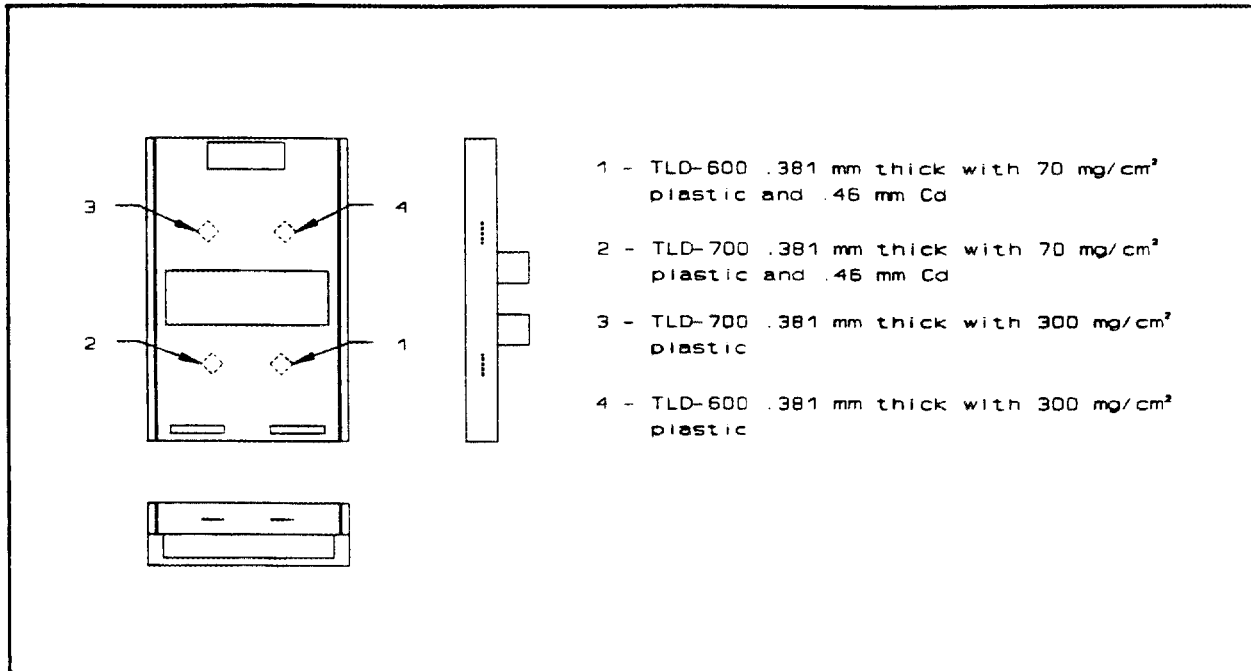


Fig. 1. Configuration of the Energy Systems beta/gamma TLD dosimeter.



**Fig. 2. Configuration of the Energy Systems neutron TLD albedo dosimeter.**

the direct thermal neutrons. The difference (total response minus the beta/gamma response) in the output of the two TLDs in each pair represents the neutron response.

The neutron dosimeter was mounted on the center front face of a  $20 \times 20 \times 10$  cm Lucite phantom. Correction factors and algorithms for evaluation of the neutron accident dose for this configuration is the same as described in Reference 2. To obtain independent information on the neutron spectrum, another dosimeter card was mounted in the center of the phantom. This was accomplished by making the phantom out of two  $20 \times 20 \times 5$  cm polymethylmethacrylate (PMMA) sections with a thin spacer placed in between (Fig. 3). The spacer, about 1-mm thick, has a slot cut the width of a dosimeter card. Part of the cut-out section is replaced to fill the void. Before insertion, one TLD pair is fitted with cadmium disks, about 1 cm in diameter and 0.46-mm thick, on each side of the card. The disk fits neatly into the hole cut in the aluminum dosimeter card to almost completely cover the TLD. To protect the dosimeter card from stray light and to make removal easier, the card and insert are wrapped in thin black plastic. In this configuration (referred to as the

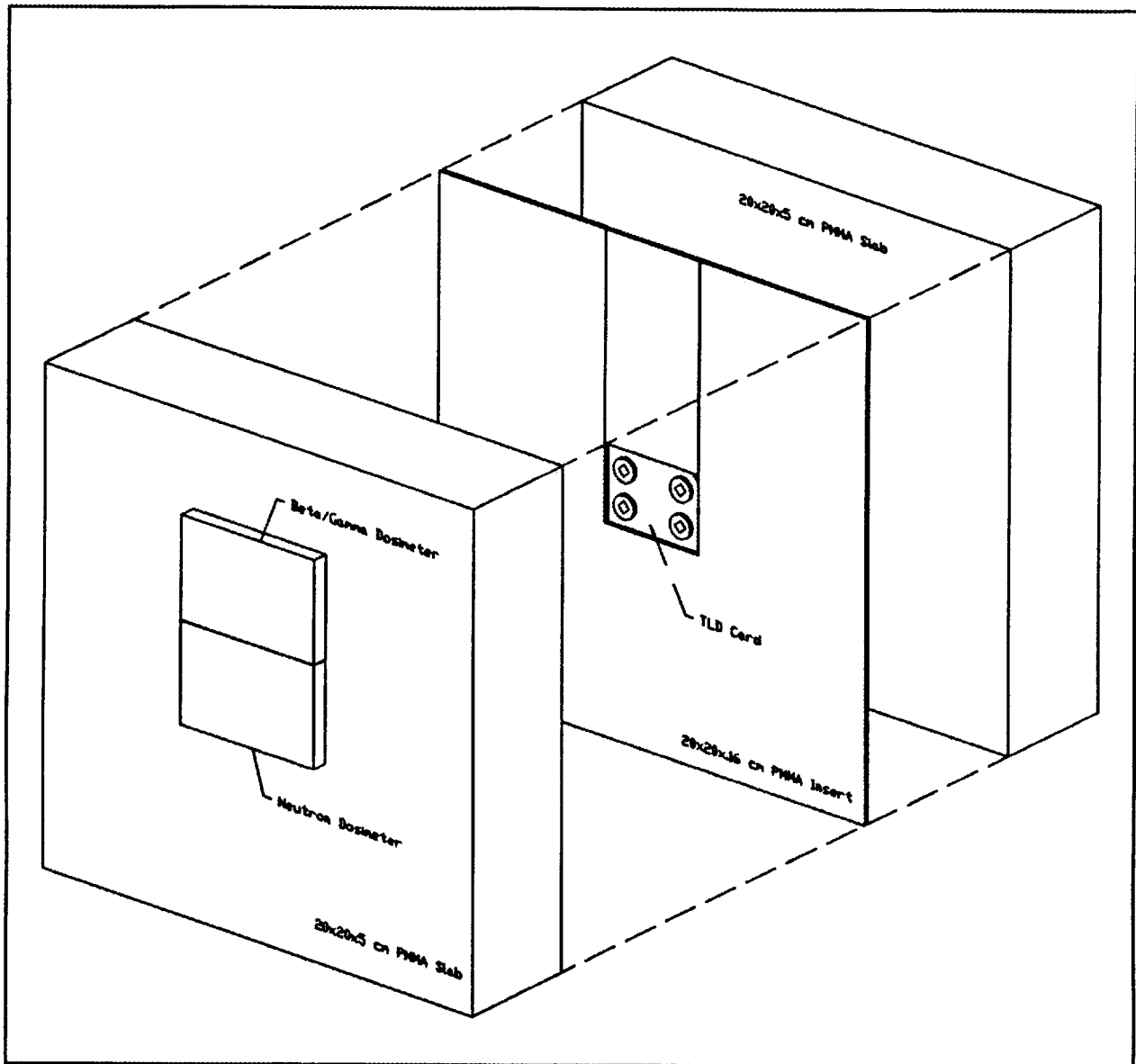


Fig. 3. Design of fixed nuclear accident dosimeter with advanced phantom design.

four-element configuration) there are four TLD 600/700 pairs—two on the front and two in the center.

Another TLD neutron dosimeter was added to the center back face of the phantom. One pair of chips on this dosimeter card had a cadmium cover over the outside to reduce sensitivity to scattered radiation. The other pair was covered by cadmium on both sides. Adding the back dosimeter results in a total of six TLD 600/700 pairs and is referred to as the six-element configuration.



### 3. DOSIMETER RESPONSE

The energy response of the TLD-600 used in the Energy Systems routine neutron dosimeter configuration has not been adequately reported in the literature, although the response of several other configurations was reported by Alsmiller and Barish,<sup>6</sup> and the energy response of a bare TLD-600 chip was calculated by Furuta and Tanaka.<sup>7-9</sup> Despite this available information, it is very difficult to ascertain the energy response for a system with a different geometry from the ones reported. Initial energy response estimates were obtained using data from the published literature. An attempt was then made to improve the calculations by modeling the system with the Monte Carlo code MCNP.<sup>10</sup>

The MCNP code is a general purpose neutron/photon transport code developed at Los Alamos National Laboratory. The code includes the necessary cross-sections from the ENDF/B-IV cross-section library for modeling neutron transport in fine detail. The code was applied to modeling the fixed accident dosimeter system without excessive geometrical detail. The TLD chips were assumed to be circular instead of square and, for the initial calculations, the holder was not modeled. The phantom was modeled with precise detail. The TLD detector was modeled as pure lithium fluoride. The code recorded the number of neutrons from a monoenergetic source which entered the TLD material. This information, obtained for several energies, was manually folded into the TLD-600 response curve published by Furuta and Tanaka.<sup>8</sup> The resulting sum was then normalized to unit response (i.e., the response per neutron). Because modeling of neutron interactions with TLDs is highly dependent upon accurately modeling the thermal neutron transport, the run time required to get reliable results from the code rapidly became excessive. In the end, it was necessary to accept higher estimated relative errors than would have been desirable, even though the estimated error was less than 10% for all the data used in the final calculations.

The calculated response curves were used in combination to predict the overall response of the system and to optimize the algorithm developed. The primary method of combining the responses is a simple linear combination.<sup>5</sup> For two TLD positions, this would result in an equation such as:

$$R_T = \alpha R_1 + \beta R_2 , \quad (1)$$

where  $R_1$  and  $R_2$  represent the neutron response of the individual TLD elements, and  $R_T$  the combined neutron response. For each additional TLD element included in the algorithm, an additional term is added. The problem now becomes one of determining the linear coefficients  $\alpha$  and  $\beta$ . A method of least squares can be applied as described by Stammers and Kingston to optimize the values so as to obtain as near a flat response as possible.<sup>11</sup> In applying this technique, the responses are expressed as  $1 \times N$  matrices, where  $N$  is the number of energy groups into which the response is broken down. Of course, the desired combined response is a  $1 \times N$  unit matrix. The above equation can then be written as:

$$R_T = \alpha R_1 + \beta R_2 = 1 . \quad (2)$$

Applying the least squares procedure, the result is:

$$\begin{vmatrix} \sum R_1^2 & \sum R_1 R_2 \\ \sum R_2 R_1 & \sum R_2^2 \end{vmatrix} \begin{vmatrix} \alpha \\ \beta \end{vmatrix} = \begin{vmatrix} \sum R_1 \\ \sum R_2 \end{vmatrix} , \quad (3)$$

where each summation is over the entire energy range of interest. The result of this operation is two equations with two unknowns. With three detector elements, the result would be three equations with three unknowns; four elements, four unknowns; etc.

If the response functions are not self-consistent, then before the coefficients can be calculated, the responses must be renormalized. This can be accomplished by exposing the detector to a well-known spectrum and evaluating the ratio of the responses. The response functions can be folded into the known spectrum to calculate the ratio of the predicted responses. The normalization factor is then the ratio of the measured response ratio to the calculated response ratio. This factor is then multiplied times each response function element. The final result can be expressed as:

$$R_n' = \alpha R_1' + \beta R_2' + \dots , \quad (4)$$

where  $R_n'$  is the resultant value of the measured quantity and  $R_i'$  is the  $i^{\text{th}}$  TLD element reading corrected for the background, photon response, individual element response, and the TLD reader calibration. The measured value corresponds to the physical quantity for which the response functions are calculated. If the response functions are for absorbed

dose, then the result is the absorbed dose. Response functions can be calculated for the fluence, absorbed dose, dose equivalent, or quality factor.

A rough estimation of the neutron spectrum can be derived using techniques such as described by Liu and Sims.<sup>12</sup> The neutron energy range is divided into three or four regions: typically thermal, low, medium, and high energies. The partitions should be selected based upon the application of the resultant spectra. For example, if the spectra are to be used for evaluating the average fluence-to-dose-equivalent conversion factor, then the partition between low and medium energies should be at about 1 keV and the partition between medium and high energies should be at about 1 MeV. These values represent critical break points in the fluence-to-dose equivalent conversion curves. Additional partitions should be in the medium energy range since in that region the slope of the conversion curve is greatest. Once the partitions are established, the average response is estimated for neutrons in each region. The detector response can then be written in the form:

$$R_i = r_{i1}\phi_1 + r_{i2}\phi_2 + r_{i3}\phi_3 + r_{i4}\phi_4, \quad (5)$$

where  $R_i$  is the response of the  $i^{\text{th}}$  TLD element,  $r_{ij}$  is the average response of the  $i^{\text{th}}$  TLD element to neutrons in energy region  $j$ , and  $\phi_j$  is the fluence in the energy region  $j$ . Using four detector elements results in four equations with four unknowns, the unknown being the neutron fluence in each of the four energy regions,  $\phi_j$ . Solving the four equations for each value of  $\phi$  results in the desired energy spectrum. A simplification can be made in the process by solving for the thermal fluence first. The difference in the cadmium- and noncadmium-covered TLDs in the front dosimeter is proportional to the thermal fluence. The response of each TLD element to the thermal fluence can then be subtracted off. The result is then three equations with three unknowns. Subtracting the thermal response first allows calculation of a smoother response curve due to the much larger responses at thermal energies than in the other energy regions.

The TLD element responses chosen for use in the algorithm are crucial to optimizing the spectral unfolding technique. In evaluating accident dosimeter results, it is normally assumed the source is a single point source. Therefore, the phantom will have a definite front and back orientation. The front dosimeter responds well to low-incident energies and allows subtraction of the thermal component. The bare (not cadmium-covered) center TLD

element provides a good response to the medium-incident energy component which is thermalized by collisions with the phantom material, and the back dosimeters provide a limited response to the higher-incident energies. If the phantom does not have a back dosimeter mounted, then the response of the cadmium-covered center TLD may be substituted to account for high-incident energies. Use of both the cadmium-covered center TLD and the back dosimeter may be of limited benefit.

Using the response curves generated in the Monte Carlo calculations, the linear combinations of the responses can be derived for each separate energy region using the least squares technique. This is accomplished by setting  $R_T$  equal to a step function for the energy region-of-interest and solving the matrix as before. The result for four energy groups is four linear equations, one for each energy group. Ideally the coefficients derived from this technique should be the same as that from Eq. (5).

Several computer codes have been developed for use with Bonner sphere systems that calculate estimated energy spectra subdivided into a greater number of energy groups than is possible by direct calculation.<sup>13</sup> Application of these codes (referred to as unfolding codes) to this system should provide the same capabilities, but will also have the same drawbacks as with Bonner spheres. For example, the calculated spectra are highly dependent upon reasonable first-guess spectrum inputs into the code. If this guess is not accurate enough, the resulting calculation may have large errors. These codes are also dependent upon an accurate, detailed response curve for each element. Direct calculation uses average element response over a large energy interval and is not highly sensitive to errors in the detailed response curves. The unfolding codes are highly dependent on the accurate value in each small energy group. The calculated response curves presented herein can be used with these codes after taking into account the effects of the calculational errors.

#### 4. CALCULATED RESULTS

Figure 4 shows the calculated monoenergetic neutron response of the front dosimeter based on the Monte Carlo model. The relative thermal responses are given in parentheses in the legend. The input for the MCNP code is given in Appendix A for each of the dosimeter positions. The calculational results for the center and back dosimeters are shown in Figs. 5 and 6. Using the above method of least squares optimization of the overall response, the  $\alpha$ ,  $\beta$ , etc., values were calculated and multiplied back into the corresponding

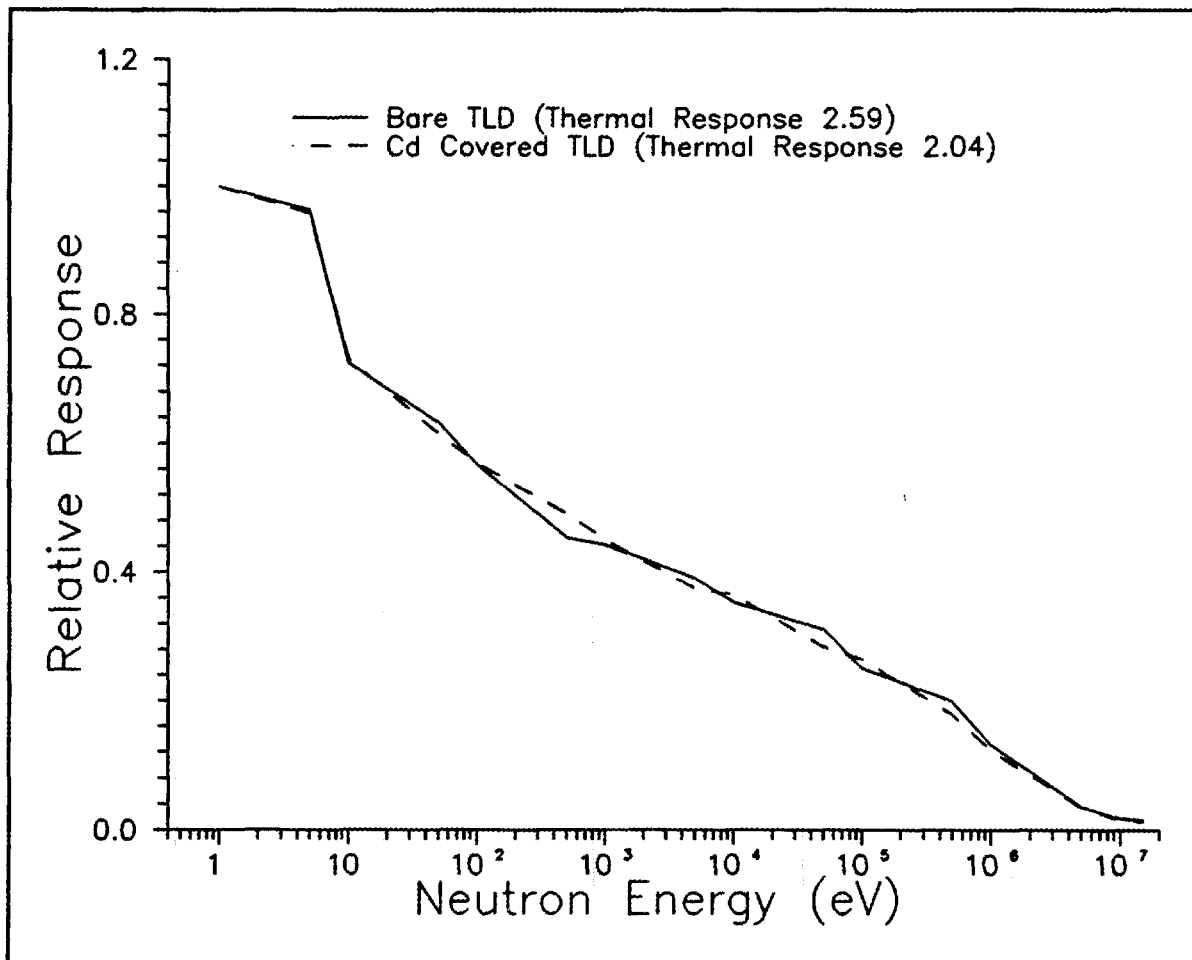
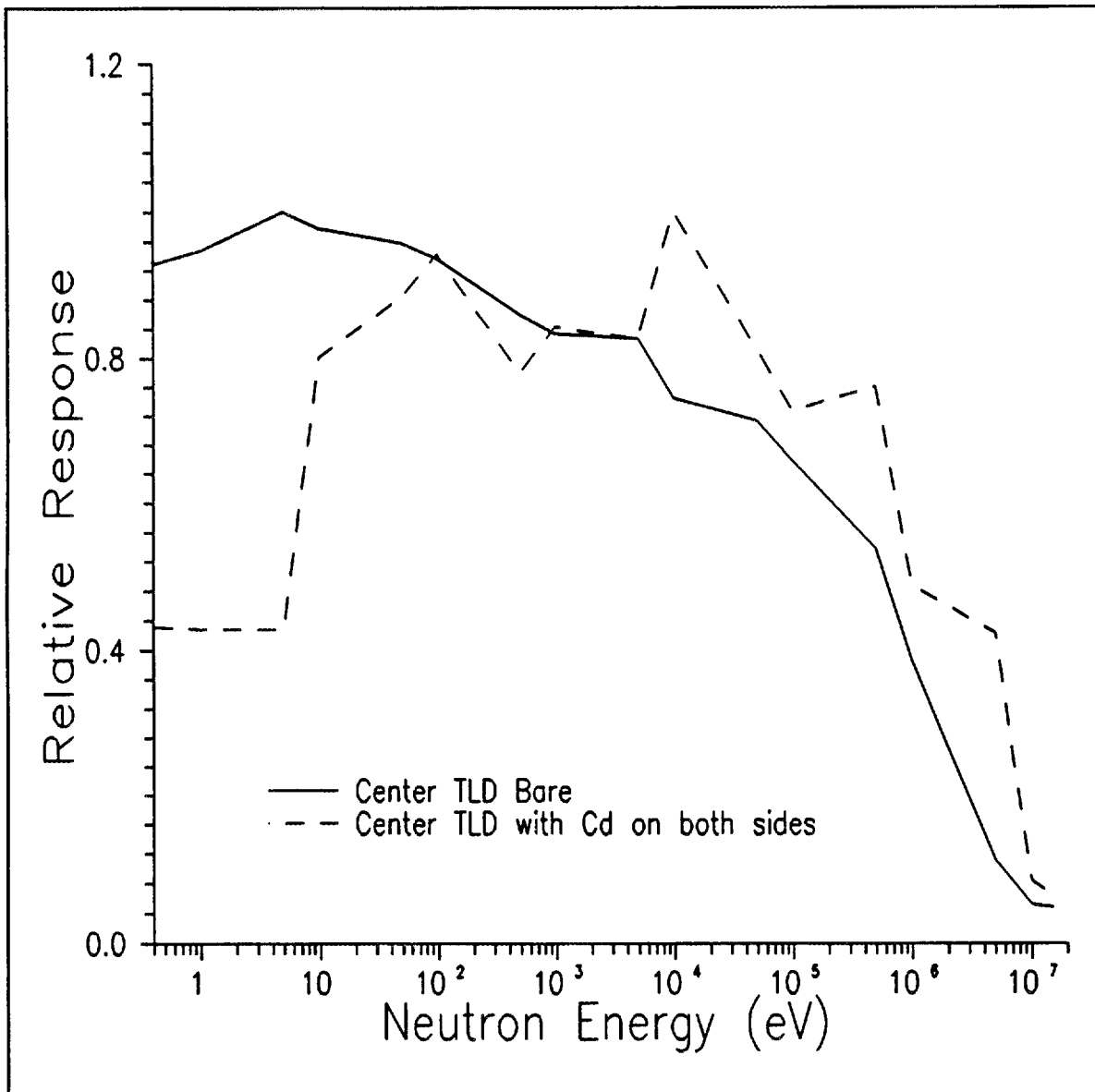
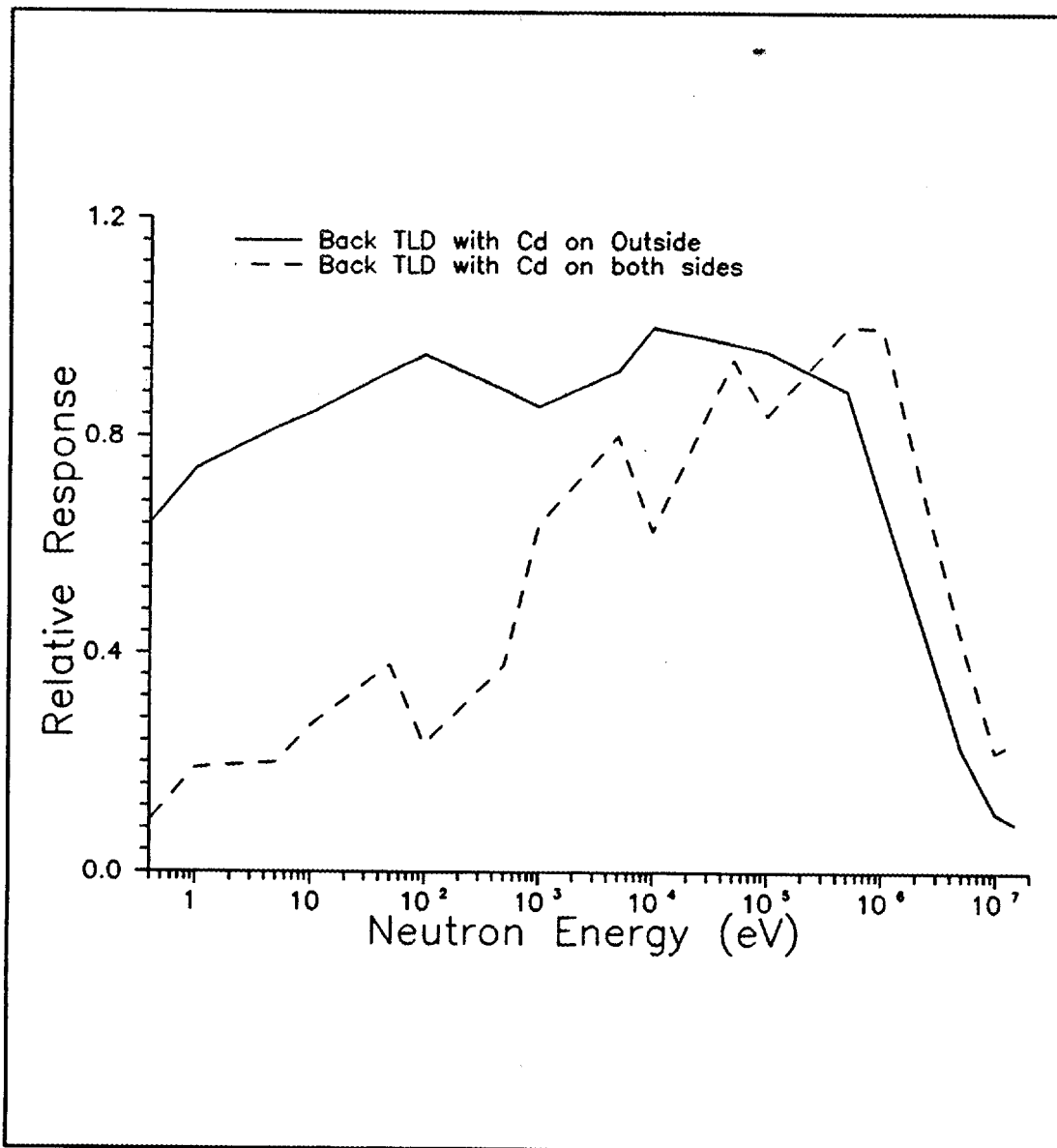


Fig. 4. Response of neutron dosimeter TLDs to monoenergetic neutrons when mounted on front of accident dosimeter as calculated by Monte Carlo code.



**Fig. 5. Response of neutron dosimeter TLD elements in center of phantom to neutrons as calculated by Monte Carlo code.**



**Fig. 6.** Response of neutron dosimeter TLD elements on back of phantom to neutrons as calculated by Monte Carlo code.

response matrices. By then summing the individual response matrices, the system response matrix was derived (Fig. 7).

To demonstrate the system response to potential accident conditions, the calculated response is folded into selected accident spectra. The resulting matrix represents the expected response of the system to each spectrum and is useful in identifying regions in which the system does not respond adequately or in which it severely overresponds. In the case of the four-element FNAD, the response is marginally adequate for most accident spectra. The overall response shown in Fig. 7 is sufficiently below 1 MeV but is greatly

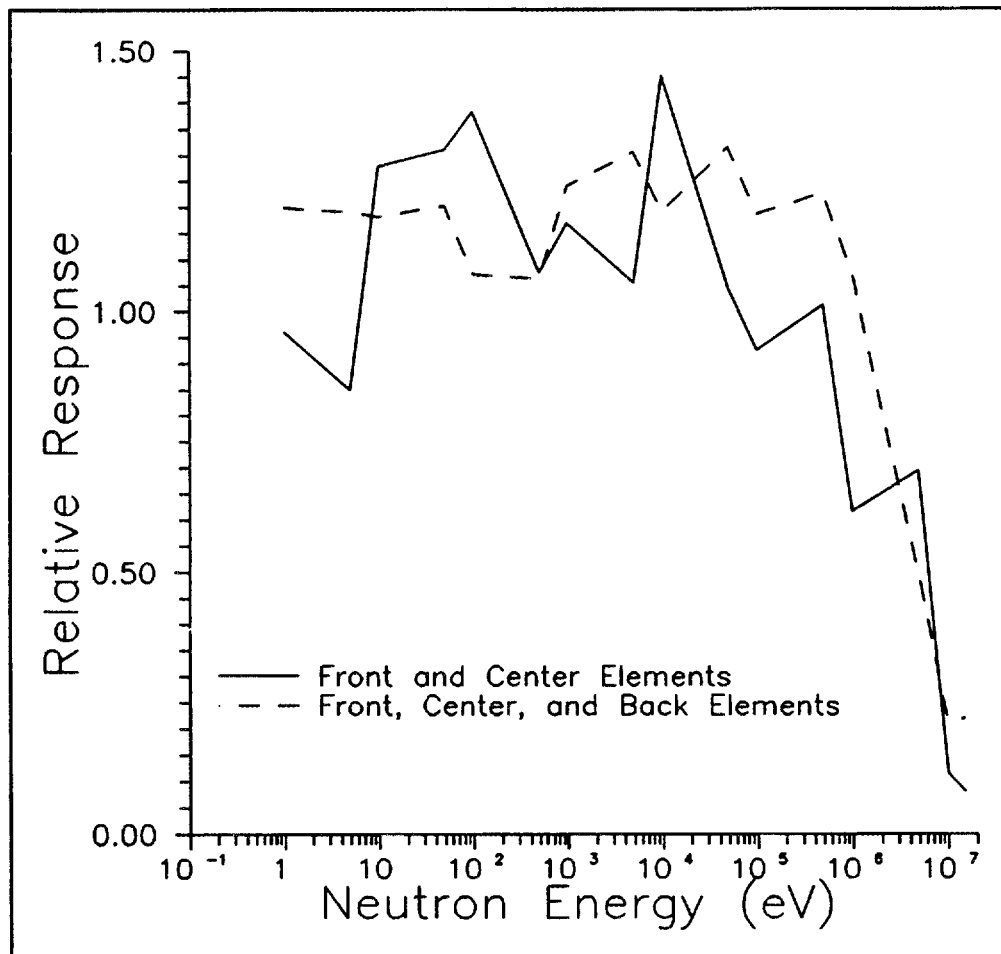


Fig. 7. Total response of complex phantom design with and without additional dosimeter on back surface.

reduced in the region above 1 MeV. The highest-energy spectrum possible during an accident is the uncollided fission spectrum shown in Fig. 8, with responses of both the four- and six-element FNADs superimposed.

The underresponse at energies above 1 MeV can be corrected by including a sulfur pellet as an activation element, although this may increase the effort required for equipment preparation and maintenance. The derived response of the system with the sulfur pellet is shown in Fig. 9. The improved responses of this configuration to various neutron spectra fluence measurements are given in Table 1.

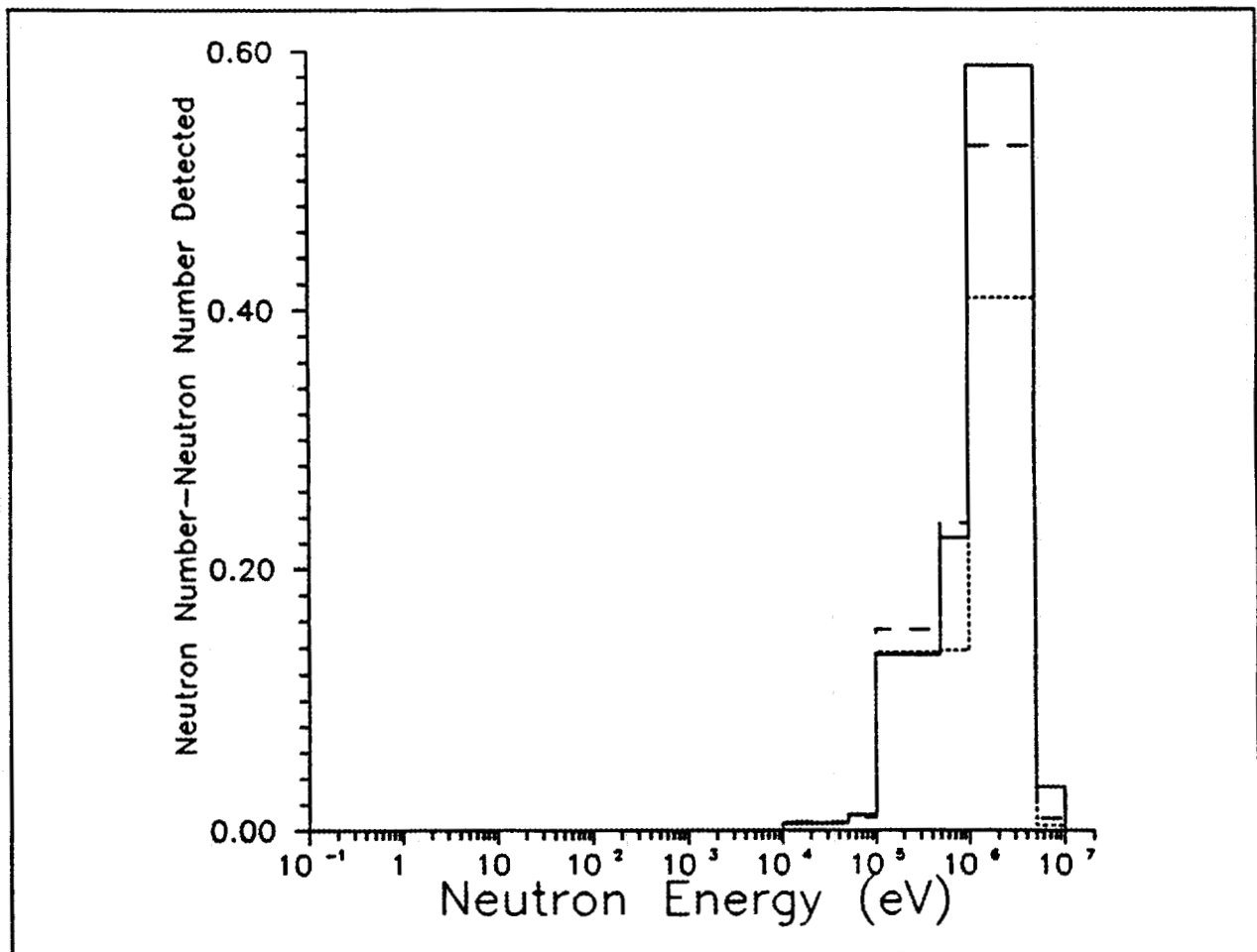
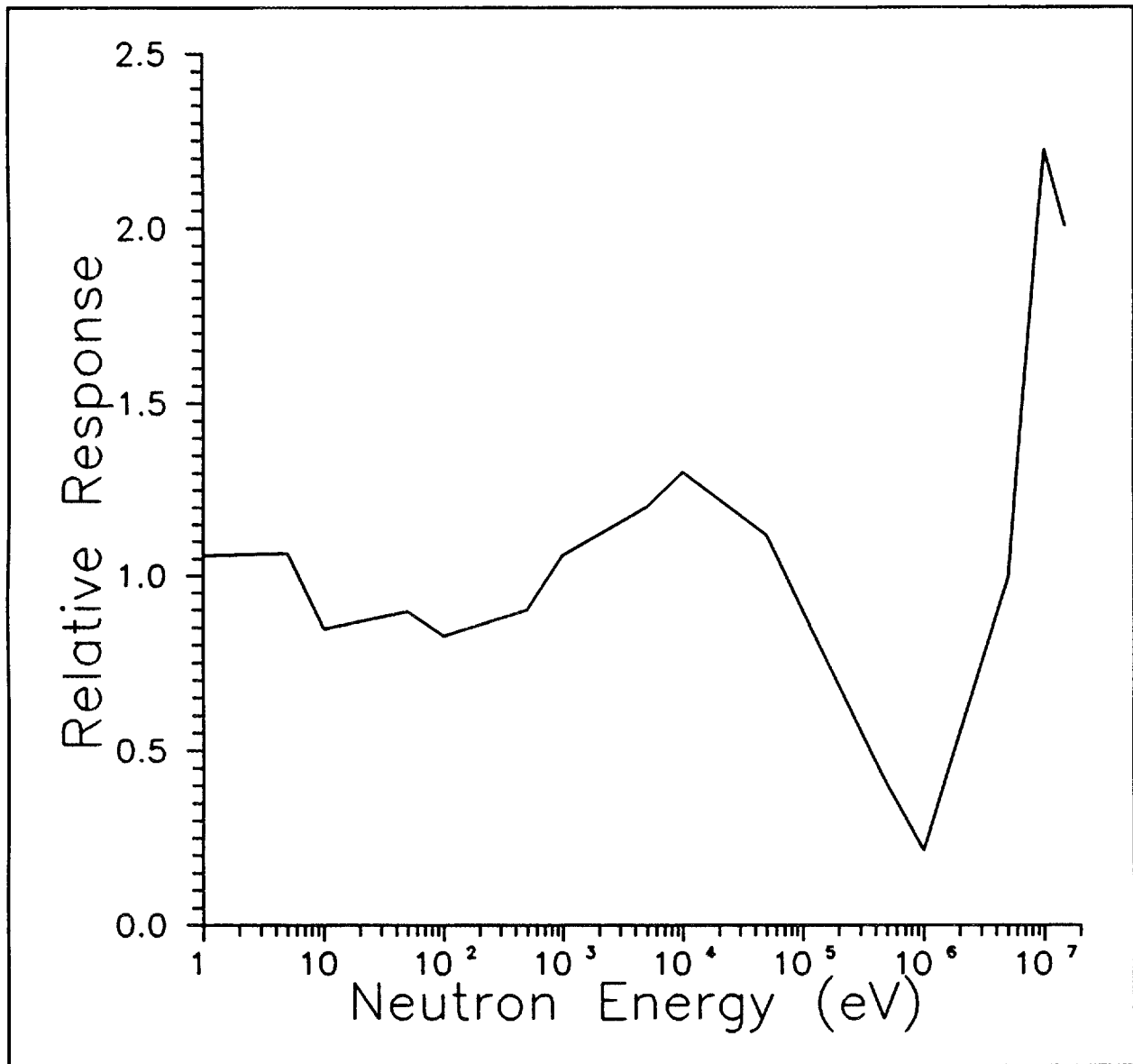


Fig. 8. Uncollided fission spectrum (solid) with four-element response (dotted) and six-element response (dashed).



**Fig. 9. Response of complex phantom design when combined with sulfur pellet response.**

**Table 1. Calculational results of the six-element-plus-sulfur fixed accident dosimeter response to neutron fluence from various sources**

	Total reference	Modeled total	1 eV to 1 keV reference	Modeled 1 eV to 1 keV	1-500 keV reference	Modeled 1-500 keV	500 keV to 15 MeV reference	Modeled 500 keV to 15 MeV
Bare Cf	1.00	0.98	0.00	0.19	0.10	0.45	0.90	0.85
Uncollided fission	1.00	0.97	0.00	0.20	0.15	0.52	0.85	0.79
D <sub>2</sub> O-moderated Cf	1.00	1.03	0.12	0.36	0.57	0.59	0.31	0.51
D <sub>2</sub> O-moderated fission through Cu	1.00	1.02	0.53	0.62	0.39	0.35	0.09	0.26
Heavily D <sub>2</sub> O-moderated fission	1.00	1.04	0.76	0.80	0.16	0.20	0.09	0.26

The neutron spectrum can be estimated by recalculating the linear coefficients as described in the previous section. Table 1 also shows the modeled results of this technique. Some care must be taken in considering these results. The system does well in identifying the major constituents of the spectrum, but does poorly in the accurate estimate of the minor constituents. When used to ascertain the general spectrum distribution, the results are consistent.

The absorbed dose, based on published spectra, is compared in Table 2 with the predicted measured result, assuming the calculated response matrix. For comparison, results are given for the same spectrum both with and without the addition of the sulfur pellet, along with the calculated percent difference. The percent difference represents a systematic error which cannot be compensated for. The statistical error and other systematic errors would be summed with this value in deriving total error. The need for the sulfur pellet is demonstrated in Table 2 for high-energy accident spectra. If only typical accident spectra are evaluated, the system can marginally meet DOE performance criteria without including a sulfur element. If isotopic neutron source spectra or unlikely uncollided fission spectra are assessed, the sulfur pellet will be necessary to meet the DOE accuracy criteria.

**Table 2. Calculational results of the fixed accident dosimeter response to neutron absorbed dose from various sources**

	Reference absorbed dose	Modeled with six-element FNAD	Percent difference	Same model with sulfur pellet	Percent difference
Bare Cf	4.60	0.87	-81	4.66	1
Uncollided fission	4.23	0.97	-77	3.77	-11
D <sub>2</sub> O-moderated Cf	2.13	1.19	-44	2.08	-2
D <sub>2</sub> O-moderated fission through Cu	7.97	9.32	17	7.23	-9
Heavily D <sub>2</sub> O- moderated fission	4.95	5.19	5	5.11	3

## 5. EXPERIMENTAL RESULTS

A small number of experimental measurements were made to test the calculational model. Unfortunately, there were no sources available that could be used to verify the response of the system to accident spectra. Californium-252 was used as a calibrated neutron source in two configurations. The system was calibrated using the broad-energy spectrum from a heavy-water-moderated  $^{252}\text{Cf}$  source. This resulted in the necessary element correction factors required for calculating the linear coefficients for the system. The system was then tested using a bare  $^{252}\text{Cf}$  source.

First the thermal neutron response components of the front two TLD sets were extracted, and the center bare (not cadmium-covered) TLD response was corrected for the estimated thermal neutron component. The corrected reading for the front cadmium-covered TLD can be expressed as:

$$G_C = G_1 - R_{T1} \frac{G_2 - G_1}{R_{T2} - R_{T1}}, \quad (6)$$

where  $G_C$  is the corrected TLD reading,  $R_{Ti}$  is the thermal response of the  $i^{\text{th}}$  TLD, and  $G_i$  is reading of the  $i^{\text{th}}$  TLD. Here TLD 1 is the bare TLD and TLD 2 is the cadmium-covered TLD. For the current calculations, the values used for the thermal responses were derived experimentally.<sup>14</sup> Responses of the front cadmium-covered TLD and the center bare TLD were both corrected, but the thermal neutron correction for the cadmium-covered center TLD and the back TLD responses were considered insignificant and left uncorrected.

The calculated response matrix for each TLD was then individually folded into the spectrum for the  $\text{D}_2\text{O}$ -moderated source. The fluence and the absorbed doses were calculated for the calibrated exposure. The calculated TLD responses to the source were then multiplied by the calibration fluence (or absorbed dose) and set equal to the product of the TLD reading and the calibration coefficient for that TLD, yielding an equation from which the calibration coefficient can be derived. These coefficients were then multiplied by the corresponding coefficients from Eq. (2). These renormalized coefficients were then used in Eq. (1).

Equation (1) was first applied directly to the results from the D<sub>2</sub>O-moderated source using the coefficients derived as described above. Due to limitations in equipment, the configuration tested consisted of the front, center, and back TLD without the cadmium between the TLD and the phantom. The estimated fluence and absorbed dose were both within 1% of the calculated response to the reference value to which the measurements were calibrated. The fluence measurement made with bare californium showed slightly better results than predicted—the system underresponded by 74% instead of a predicted 92% for fluence. The absorbed dose measurement was quite different than predicted. The system overresponded to the absorbed dose by 25% instead of the predicted 49% underresponse. Since the fluence-to-absorbed-dose conversion factor at high energies (such as the high average energy from a bare californium source) is much larger than at medium and low energies, a small error above the predicted value in fluence can result in a large error in absorbed dose. The results from the above test are consistent with a small error in the response functions at high energies. This error is less likely in the six-element model and will probably not be a factor when the sulfur pellet is used.

In order to evaluate the effect from exposure to angles other than normal, the system was exposed to the bare californium source at angles of 0, 30, 60, and 85°. The results were normalized to unit response at 0° angle (normal to the front surface). As can be seen in Figs. 10 and 11, the change in response is similar for most of the TLD positions but shows a large change for the back dosimeter. The TLD on the back of the phantom, without cadmium, shows the same change as the front and center TLDs up to 60°. The cadmium-covered TLD on the back shows a marked difference for all angles other than normal. Because of this effect, the response of the cadmium-covered TLD on the back of the phantom is not recommended for use in the calculations and the final algorithm.

Several measurements and calculations remain to be accomplished. The system will be tested with all six TLD elements in the proper configuration and with simulated data from a sulfur pellet. There is also the possibility of testing the system with several monoenergetic neutron sources in the future. This data will be very useful in verifying the calculation results and improving the response curves. If the high-energy response remains in question, tests may be performed with other high-energy neutron sources (such as PuBe and AmBe).

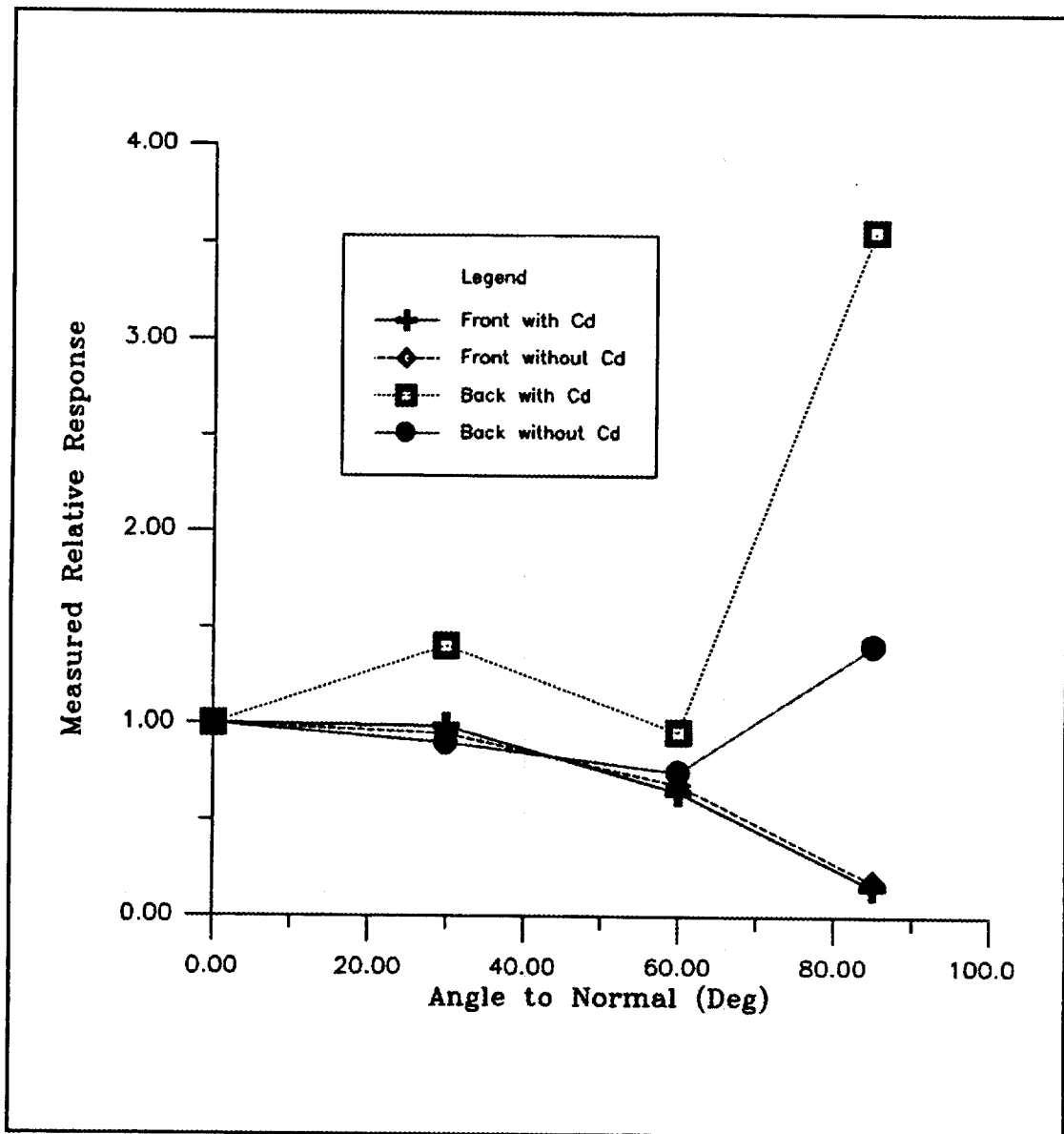


Fig. 10. Response of TLDs at front and back positions as a function of angle.

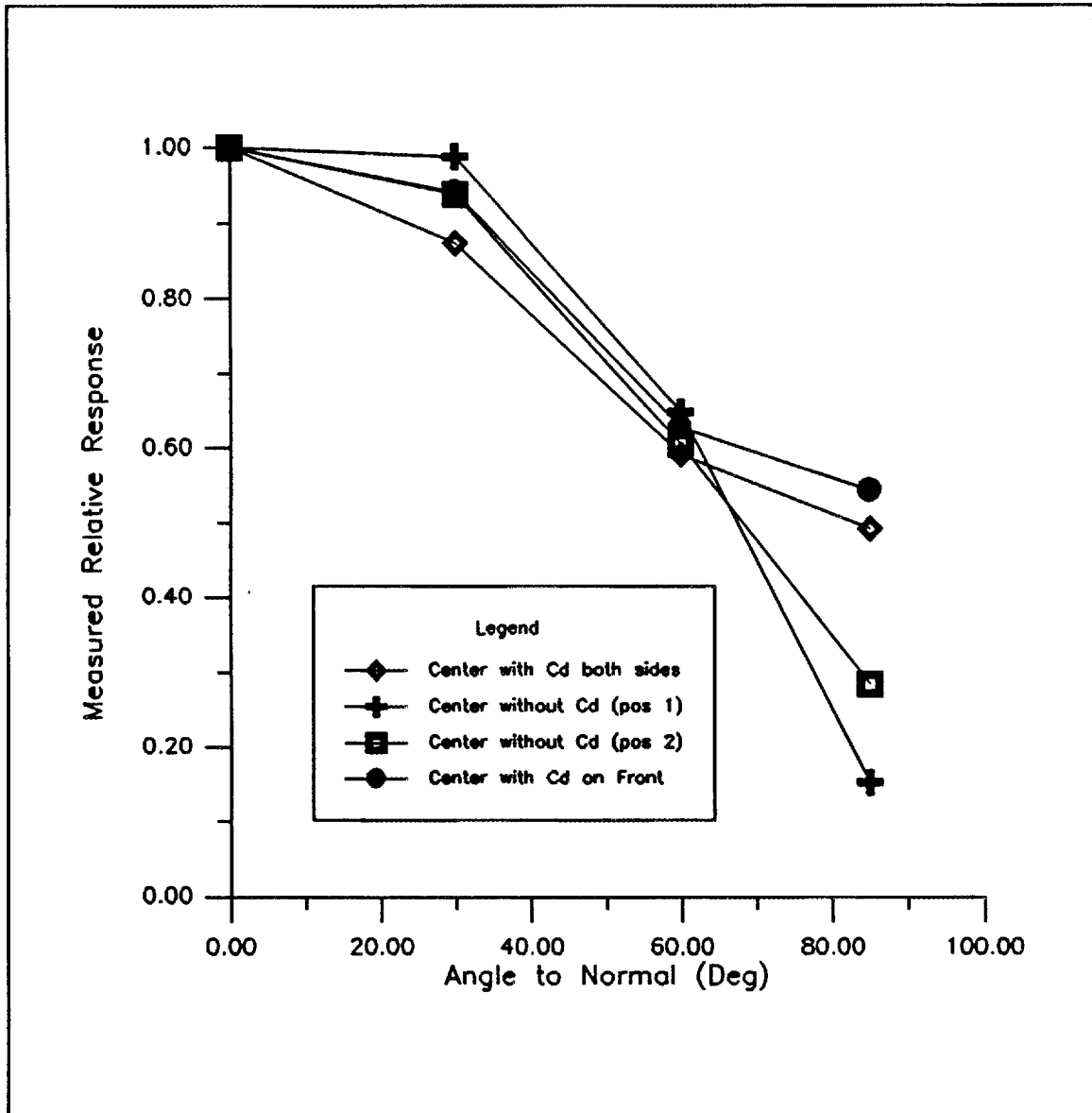


Fig. 11. Response of TLDs at center position as a function of angle.

## 6. CONCLUSIONS

Design and calculations for using a TLD-based system for a FNAD have been completed with sufficient results to have proof of principle. The calculations have required a large amount of computational time and as yet have not been adequate to reduce the uncertainty to the desired level, primarily because of the thermal response of the TLD-600 material and the difficulty in reducing the error in energy down-scatter calculations to the thermal region. This makes calculations of the thermal response difficult and lengthy. Calculations of the response to higher-energy neutrons is more straightforward; but, since thermal neutrons play a central role in a system with moderation or one which relies on albedo detection, the same uncertainties still have a significant effect. More calculational time will be available in the near future which may reduce the discrepancies identified in this report.

A mathematical method of least squares has been applied in order to optimize the linear combination of several dosimeter elements in a manner that is straightforward and has the benefit of analyses of measurement results being simple and precise. The results of this technique are highly dependent on the accurate knowledge of the response curves for each dosimeter element. This information may be derived by the aforementioned calculational technique, by experimental measurement, or by a combination of the two. In this application, the derived results have been totally dependent upon calculations, but will be combined with experimental data in the near future.

The experimental results thus far show considerable discrepancy with the calculations. These discrepancies are greatly amplified by the fact that the measurements were made with a source with a high average energy even above the highest expected from a plausible nuclear accident geometry. Also, the measurements were made without using two of the elements which were later included in the calculations to improve accuracy at those energy levels. It is expected that further evaluation of the system will produce better results with those elements included.

The application of TLDs to accident dosimetry shows great promise for the future. A single TLD mounted on a small phantom can give reasonable results if the accident neutron spectrum can be estimated from information provided about the configuration of the fissionable material and the surrounding shielding. Information from the

neutron-to-gamma ratio and the magnitude of the thermal neutron component can aid in evaluating the proper spectrum. This system can be improved by inserting an additional TLD set in the center of the phantom. The moderation provided by the phantom is similar to that from a Bonner sphere and can be used in a similar fashion. By combining the results from TLDs in the center and front of the phantom, a crude spectrum can be derived. More importantly, the fluence, absorbed dose, and the dose equivalent can be calculated directly without the need to know the neutron spectrum accurately. Some additional advantages include the extensive range of the TLD technique and the sensitivity of TLDs to neutrons. The TLD system described should be able to analyze accidents with absorbed doses at the detector position in the range of 10 mrad to 10,000 rad without any significant loss in accuracy. Additional improvements can be made to the system by placing an additional dosimeter on the back of the phantom, supplementing the TLD results with a sulfur pellet, and applying spectrum unfolding techniques to the system (such as those used with standard Bonner sphere spectrometer systems). The resulting error in this technique is due to the fact that the responses are smooth curves rather than step functions. The response curves for each energy region, therefore, have some residual sensitivity to neutrons in other energy groups. This results, in general, in an overestimate of the neutrons in energy regions with small neutron populations and in the sum of the energy regions, which is significantly higher than estimated by the total response. This can be clearly seen in the results for bare californium and uncollided fission spectra in Table 1. The low-energy group has a neutron population near zero, but the model calculates about twenty due to bleedover from higher energies. This problem may be significantly reduced by reducing the uncertainty in the original response curve calculations, which should result in smoother curves and could be done with a larger number of energy groupings.

In order to move the development of this system from the proof of principle to full application, the calculation of the response curves must be improved, additional measurements must be made, and it is recommended that the system be tested in a simulated accident neutron field. When the system has been proven under these conditions, it will provide a unique, cost-effective alternative to the current nuclear accident dosimetry systems without use of special nuclear materials or a large investment in equipment and manpower.

## REFERENCES

1. *Dosimetry for Criticality Accidents: A Manual*, Technical Reports Series 211, Atomic Energy Agency, Vienna, 1982.
2. W. H. Casson, G. T. Mei, and M. A. Buckner, *Test and Recommendations for the Application of the CEDS Dosimeter to Nuclear Accident Dosimetry*, ORNL-6667, Martin Marietta Energy Systems, Inc., Oak Ridge Natl. Lab. (to be published).
3. "Radiation Protection for Occupational Workers," DOE Order 5480.11 (1988).
4. M. Anschalom and R. S. Sanna, "Applications of Bonner Sphere Detectors in Neutron Field Dosimetry," *Rad. Prot. Dos.* 10(1-4), 89 (1985).
5. E. Piesch and B. Burghardt, "Measurement of Neutron Field Quantities Using the Single Sphere Albedo Technique," *Proc. of the Fifth Symposium on Neutron Dosimetry*, Vol. 1, p. 403, Munich (1985).
6. R. G. Alsmiller, Jr. and J. Barish, *The Calculated Response of Albedo-Neutron Dosimeters to Neutrons with Energies  $\leq 400$  MeV*, ORNL/TM-3984, Martin Marietta Energy Systems, Inc., Oak Ridge Natl. Lab., December 1972.
7. Y. Furuta and S. Tanaka, "Response of  $^6\text{LiF}$  and  $^7\text{LiF}$  Thermoluminescence Dosimeters to Fast Neutrons," *Nucl. Instr. and Meth.* 104, 365-374 (1972).
8. Y. Furuta and S. Tanaka, "Revised Energy Responses of  $^6\text{LiF}$  and  $^7\text{LiF}$  Thermoluminescence Dosimeters to Neutrons," *Nucl. Instr. and Meth.* 140, 395-396 (1977).
9. Y. Furuta and S. Tanaka, "Usage of a Thermoluminescence Dosimeter as a Thermal Neutron Detector with High Sensitivity," *Nucl. Instr. and Meth.* 133, 495-499 (1976).
10. J. F. Briesmeister, ed., *MCNP 4 - Monte Carlo Neutron and Photon Transport Code System*, ORNL-RSIC-CCC-200A/B, Martin Marietta Energy Systems, Inc., Oak Ridge Natl. Lab., July 1992.
11. K. Stammers and S. A. Kingston, "The Use of Metal Filters to Flatten the Energy Response of  $\text{CaSO}_4:\text{Tm}$  TL Dosemeters, and to Provide Spectral Information," *Rad. Prot. Dos.* 36, 23-29 (1991).
12. J. C. Liu and C. S. Sims, "Performance Evaluation of a New Combination Personnel Neutron Dosemeter," *Rad. Prot. Dos.* 32, 33-43 (1990).
13. J. T. Routti and J. V. Sandberg, "Unfolding Activation and Multisphere Detector Data," *Rad. Prot. Dos.* 10(1-4), 103-110 (1985).

14. M. A. Buckner, *Improving Neutron Dosimetry Using Bubble Detector Technology*, ORNL/TM-11916, Martin Marietta Energy Systems, Inc., Oak Ridge Natl. Lab., February 1993.

## **APPENDIX A**

**Sample Input File for MCNP Code**

Appendix A is a sample input file for the MCNP code used to calculate the responses of the various elements of the FNAD dosimeter. This file calculates the response of the TLDs on the back of the dosimeter, both bare and with cadmium between the TLD and the phantom, to neutrons with a single energy of 5 MeV.

## Third Problem - Complex Phantom Response/Back Dosimeter

1 1 -.92 -1 2 -3 4 -5 6 imp:n=1  
 2 0 10 -23 imp:n=0  
 3 0 3 -23 2 -1 imp:n=0  
 4 0 -4 -23 2 -1 imp:n=0  
 5 0 5 -23 2 -1 -3 4 imp:n=0  
 6 0 -6 -23 2 -1 -3 4 imp:n=0  
 7 0 1 -7 -23 imp:n=1  
 8 2 -2.64 8 -9 -19 imp:n=1  
 9 2 -2.64 8 -9 -20 imp:n=1  
 10 2 -2.64 8 -9 -21 imp:n=1  
 11 2 -2.64 8 -9 -22 imp:n=1  
 12 4 -8.64 7 -8 -15 imp:n=1  
 13 4 -8.64 7 -8 -16 imp:n=1  
 14 0 7 -8 -17 imp:n=1  
 15 0 7 -8 -18 imp:n=1  
 16 0 8 -9 19 -15 imp:n=1  
 17 0 8 -9 20 -16 imp:n=1  
 18 0 8 -9 21 -17 imp:n=1  
 19 0 8 -9 22 -18 imp:n=1  
 20 0 9 -10 -15 imp:n=1  
 21 4 -8.64 9 -10 -16 imp:n=1  
 22 4 -8.64 9 -10 -17 imp:n=1  
 23 0 9 -10 -18 imp:n=1  
 24 3 -2.7 -11 12 -13 14 7 -10 15 16 17 18 imp:n=1  
 25 0 11 7 -10 -23 imp:n=1  
 26 0 -12 7 -10 -23 imp:n=1  
 27 0 13 -11 12 7 -10 -23 imp:n=1  
 28 0 -14 -11 12 7 -10 -23 imp:n=1  
 29 0 -2 -3 4 -5 6 24 imp:n=1  
 30 0 -24 -23 imp:n=0  
 31 0 23 imp:n=0  
 32 0 -2 24 -23 3 imp:n=1  
 33 0 -2 24 -23 -4 imp:n=1  
 34 0 -2 24 -23 -3 4 5 imp:n=1  
 35 0 -2 24 -23 -3 4 -6 imp:n=1

1 px 0  
 2 px -10  
 3 py 10  
 4 py -10  
 5 pz 10  
 6 pz -10  
 7 px .5  
 8 px .531  
 9 px .569  
 10 px .6

```
11 py 2.15
12 py -2.15
13 pz 1.55
14 pz -1.55
15 c/x 1.3 .75 .45
16 c/x 1.3 -.75 .45
17 c/x -1.3 .75 .45
18 c/x -1.3 -.75 .225
19 c/x 1.3 .75 .255
20 c/x 1.3 -.75 .225
21 c/x -1.3 .75 .225
22 c/x -1.3 -.75 .255
23 so 20
24 px -12
```

```
mode in
sdef sur=24 pos -12 0 0 rad d1 erg=5.0 nrm 1 dir=1 ara=400 ccc=29
si1 0 20
m1 1001.04 =.0805 6012.10 -.5999 8016.04 -.3196
m2 3006.10 -.2405 9019.03 -.7595
m3 13027.04 -1
m4 48000.01 1
f4:n 8 9 10 11
e4 .000000414 .000005 .00001 .00005 .0001 .0005 .001 .005
    .01 .05 .1 .5 1 5 10 15
cut:n 1.e16 1.0e-11 .01
nps 50000000
print
```

## DISTRIBUTION

1. A. B. Ahmed
2. J. F. Alexander
3. B. A. Berven
4. J. S. Bogard
5. R. S. Bogard
- 6-10. W. H. Casson
11. S. W. Croslin
12. E. C. Crume
13. W. L. DeRossett
14. T. C. Dodd
15. C. M. Hopper
16. J. B. Hunt
17. G. D. Kerr
18. E. Maples
19. K. L. McMahan
- 20-24. G. T. Mei
25. W. F. Ohnesorge
26. P. S. Rohwer
27. C. S. Sims
28. M. Thein
29. Central Research Library
30. ORNL Technical Library, Y-12
- 31-32. Laboratory Records Dept.
33. Laboratory Records—RC
34. ORNL Patent Section
35. Office of Assistant Manager for Energy Research and Development, Department of Energy, Oak Ridge Operations, P.O. Box 2001, Oak Ridge, TN 37831-8600
- 36-37. Office of Scientific and Technical Information, P.O. Box 62, Oak Ridge, TN 37831
38. A. Bassett, Department of Energy, Oak Ridge Operations, P.O. Box 2008, Oak Ridge, TN 37831-6269
39. W. K. Crase, Westinghouse Savannah River Company, Savannah River Site, Bldg. 735A, Aiken, SC 29802
40. J. F. Higginbotham, Radiation Center, Oregon State University, Corvallis, OR 97331
41. H. H. Hsu, Los Alamos National Laboratory, P.O. Box 1663-G761, Los Alamos, NM 87545
42. J. W. Poston, Texas A&M University, Department of Nuclear Engineering, College Station, TX 77843
43. R. B. Schwartz, National Institute of Standards and Technology, Bldg. 235, Gaithersburg, MD 20899
44. G. G. Simons, Engineering Experiment Station, Durland Hall, Kansas State University, Manhattan, KS 66506-5103